



Copyright Infopro Digital Limited 2020. All rights reserved. You may share using our article tools. This article may be printed for the sole use of the Authorised User (named subscriber), as outlined in our terms and conditions. <https://www.infopro-insight.com/termsconditions/insight-subscriptions>

Research Paper

Network sensitivity of systemic risk

**Amanah Ramadiah,¹ Domenico Di Gangi,²
D. Ruggiero Lo Sardo,³ Valentina Macchiati,^{2,4}
Tuan Pham Minh,⁵ Francesco Pinotti,⁶
Mateusz Wilinski,^{2,7} Paolo Barucca¹ and
Giulio Cimini^{8,9,10}**

¹Department of Computer Science, University College London, London WC1 E6BT, UK; email: amanah.ramadiah.14@ucl.ac.uk

²Scuola Normale Superiore, Piazza dei Cavalieri 7, 56126 Pisa, Italy; emails: domenico.digangi@sns.it, valentina.macchiati@sns.it

³Medical University of Vienna, Spitalgasse 23, 1090 Vienna, Austria; email: losardor@gmail.com

⁴Department of Physics, University of Turin, Via Pietro Giuria 1, 10125 Torino, Italy; email: valentina.macchiati@sns.it

⁵N/A; email: physicsidea@gmail.com

⁶INSERM, Sorbonne Université, Institut Pierre Louis d'Épidémiologie et de Santé Publique (IPLESP), 75012 Paris, France; email: francesco.pinotti@iplesp.upmc.fr

⁷Faculty of Physics, University of Warsaw, Pasteura 5, 02-093 Warsaw, Poland; email: mateusz.wilinski@fuw.edu.pl

⁸Department of Physics, University of Rome Tor Vergata, Via della Ricerca Scientifica 1, 00133 Rome, Italy

⁹IMT School for Advanced Studies, Piazza San Francesco 19, 55100 Lucca, Italy

¹⁰Institute for Complex Systems (CNR), UOS Sapienza, Piazzale Aldo Moro 2, 00185 Rome, Italy; email: giulio.cimini@roma2.infn.it

(Received July 26, 2019; revised December 22, 2019; accepted May 7, 2020)

ABSTRACT

A growing body of studies on systemic risk in financial markets has emphasized the key importance of taking into consideration the complex interconnections among financial institutions. Much effort has been put into modeling the contagion dynamics

of financial shocks and into assessing the resilience of specific financial markets, either using real network data, reconstruction techniques or simple toy networks. Here, we address the more general problem of how shock propagation dynamics depend on the topological details of the underlying network. To this end, we consider different realistic network topologies, all consistent with balance sheet information obtained from real data on financial institutions. In particular, we consider networks of varying density and with different block structures. In addition, we diversify in the details of the shock propagation dynamics. We confirm that the systemic risk properties of a financial network are extremely sensitive to its network features. Our results can aid in the design of regulatory policies to improve the robustness of financial markets.

Keywords: financial networks; systemic risk and contagion; DebtRank; network reconstruction; mesoscale structure.

1 INTRODUCTION

The crises that hit the financial world in the last two decades led scientists and regulators to rethink, with a systemic perspective, the approach used to assess market risk, with an increased interest in the entangled structure of financial relationships (Acemoglu *et al* 2015; Allen and Gale 2007; Allen *et al* 2014), its role in the potential propagation of risk (Gai and Kapadia 2010) and its consequences for risk management and macroprudential regulation (Battiston *et al* 2016b; Haldane and May 2011). A common denominator that has emerged from the many empirical works on systemic risk is the importance of considering the role of the structure of financial dependencies (Boss *et al* 2004; Cocco *et al* 2009; Georg 2013; Nier *et al* 2007). It has also become clear that centrality measures in financial networks can be crucial to identify systemically important financial institutions (Battiston *et al* 2012).

While the evidence of the role of interconnections and the need for their direct measurement or reconstruction (Anand *et al* 2018) has grown, at the same time, the research on designing novel and more realistic systemic risk mechanisms has greatly developed in recent years. Starting with the seminal works on clearing mechanisms (Eisenberg and Noe 2001) and default contagion (Furfine 2003), a growing number of extensions have been introduced (Acharya *et al* 2017; Amini *et al* 2016; Benoit *et al* 2017; Caccioli *et al* 2018), and we now have methods ranging from the seminal default contagion approaches to distress contagion, such as DebtRank centrality (Battiston *et al* 2012) and network valuation (Barucca *et al* 2016). These kinds of network methodologies are nowadays implemented in stress tests and stability analysis performed by central banks (Bardoscia *et al* 2019; Covi *et al* 2019). Therefore, the current scientific challenge is no longer to generically quantify systemic risk, but

to be able to understand in more detail the interplay between systemic risk measures and network structures, as different contagion mechanisms may yield different risks and vulnerabilities depending on the underlying network structure. Only with this increased level of understanding can specific regulatory solutions to improve the structure of the system and reduce risk become reliable. To this end, it is essential to understand which features of a financial network make it more or less resilient to systemic risk.

One of the first contributions in this direction was the work of Gai and Kapadia (2010), who showed that random Erdős–Rényi networks are “robust-yet-fragile”: the probability of contagion is maximal for intermediate network densities, whereas the amount of systemic losses monotonically increases with the network connectivity. Further, Mastromatteo *et al* (2012) showed that, under the Furfine dynamics, sparse Erdős–Rényi networks in general lead to more defaults than very dense networks. Roukny *et al* (2013) noted that no single topology can always lead to the lowest risk levels (in particular, scale-free networks can be both more robust and more fragile than Erdős–Rényi architectures). León and Berndsen (2014) argued that modular scale-free architectures can favor robustness, whereas Montagna and Lux (2017) pointed out that the dependence of systemic risk on the density will change if shocks are correlated. Hurd *et al* (2017) observed that, under the Gai and Kapadia dynamics, degree assortativity can strongly affect the course of contagion cascades (Hurd *et al* 2017). With regard to the DebtRank dynamics, Bardoscia *et al* (2017) showed that the stability of the system decreases monotonically with the link density due to the presence of cycles, whereas Krause *et al* (2019) recently pointed out that degree assortativity correlates well with the level of systemic risk.

In this work, for the first time, we generalize one of the most consolidated methods for reconstructing realistic financial networks (Anand *et al* 2018) for the case of weighted heterogeneous networks with core–periphery and modular block structures, respectively. Further, we introduce a robust and efficient network sensitivity methodology that explores a range of weighted financial networks with varying density (from extremely sparse low-density networks to complete ones) and applies two paramount models of both default contagion and distress contagion, displaying the significant differences in relative losses that can arise from different network structures, shocks applied and contagion mechanisms.

2 METHODOLOGY

In this section, we explain the two-step procedure we use in our framework. In a nutshell, first we generate a reconstructed financial network with some key characteristics, and then we run shock propagation dynamics, Furfine and DebtRank algorithms, over it in order to assess its level of systemic risk.

2.1 Data

We base our reconstruction of financial (specifically, interbank) networks on Bankscope data (Battiston *et al* 2016a) containing the balance sheet of the 100 largest European banks. In particular, we have information about the interbank assets A_i , the interbank liabilities L_i and the equities E_i of each i of these banks, and we consider data for the years 2008 and 2013 (ie, during and after the global financial crisis) (Angelini *et al* 2011). We recall that the equity of a bank is the difference between its total positive positions and its total obligations to creditors. When the equity is positive, the bank is solvent; otherwise, it goes bankrupt (defaults) because it is not able to refund its debts. Since the chosen group of banks is not an isolated system, interbank assets and liabilities do not sum up to the same value. In order to have a closed system, we rescale them such that $\sum_j A_j = \sum_j L_j$.

2.2 Network generation

In the literature on financial networks, interbank markets are typically reconstructed from balance sheet data (before being tested for systemic risk) (Anand *et al* 2018). Here, we use and generalize the approach of Cimini *et al* (2015) to generate reconstructed financial networks (that is, compatible with balance sheet information) with different underlying topologies. The method is grounded in statistical physics concepts applied to networks (see further details in Squartini *et al* (2018) and Cimini *et al* (2019)).

To create a single network instance, we first generate an unweighted directed graph by drawing each link $i \rightarrow j$ independently with probability

$$p_{i \rightarrow j} = \frac{z A_i L_j}{1 + z A_i L_j}, \quad (2.1)$$

where $z \in (0, \infty)$ is a parameter that controls the density of the network. Indeed, since the values of assets and liabilities are given, this probability is an increasing function of z ; hence, the link density of the network is proportional to the parameter z .

After the link generation process, we assign a weight to each realized link as follows:

$$w_{i \rightarrow j} = \frac{A_i L_j}{\Omega p_{i \rightarrow j}} a_{i \rightarrow j}, \quad (2.2)$$

where the adjacency matrix element $a_{i \rightarrow j}$ equals 1 if the draw of (2.1) was successful (and zero otherwise), and $\Omega = [(\sum_j A_j)(\sum_j L_j)]^{1/2}$. The final result is a weighted directed network given by the corresponding adjacency matrix \mathbf{W} , whose entries are the weights $\{w_{i \rightarrow j}\}$. In the economic network literature, this matrix is referred to as the asset matrix, while its transpose is called the liability matrix.

Overall, this recipe is used to generate an ensemble of networks, having the property that the interbank assets and liabilities of each bank are constrained in probability to their real values as

$$\left\langle \sum_j w_{i \rightarrow j} \right\rangle = A_i \quad \text{and} \quad \left\langle \sum_j w_{j \rightarrow i} \right\rangle = L_i$$

(here, $\langle \cdot \rangle$ denotes the average over the ensemble). Note that by using (2.1) we allow the formation of self-loops in the network, because some of the top European banks do represent banking groups with an internal flow of money. The alternative possibility would be to use the RAS algorithm to get rid of them, while preserving the imposed constraints (Squartini *et al* 2017).

Importantly, the distribution of assets and liabilities across banks is heterogeneous, and with such an input our network construction method automatically generates a core–periphery structure, independently of the network density. In order to tune this outcome, we introduce a generalization of (2.1):

$$p_{i \rightarrow j} = \frac{z(A_i L_j)^\phi}{1 + z(A_i L_j)^\phi}, \quad \phi \in [0, 1]. \tag{2.3}$$

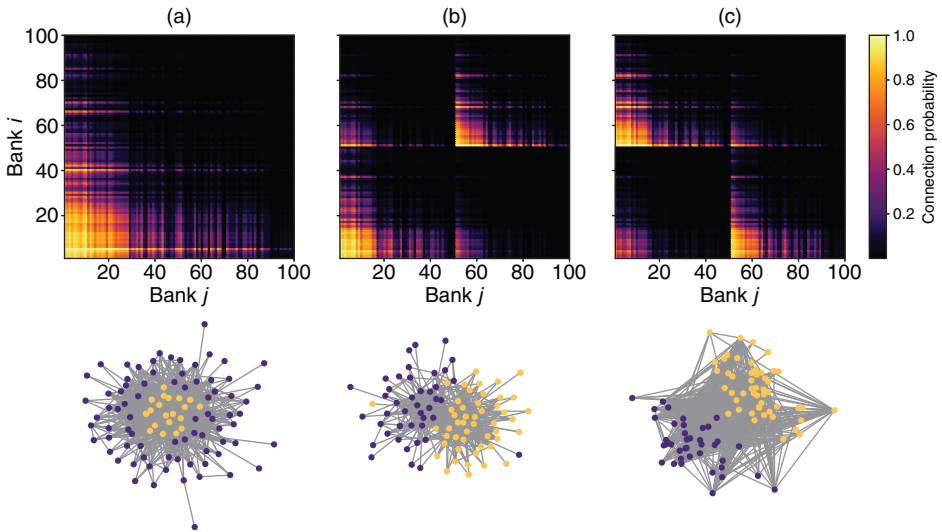
The new parameter ϕ allows us to model a wide range of network topologies (for fixed z), interpolating between the fitness-induced configuration model and the Erdős–Rényi random graph as the two limits $\phi = 1$ and $\phi = 0$, respectively. Besides, weights assignment as for (2.2) satisfies the constraints on the interbank assets and liabilities of each bank whatever the choice of connection probabilities $\{p_{i \rightarrow j}\}$.

2.3 Block structure

The network reconstruction method just illustrated allows for the exploration of different network structures. To this end, we can further decompose the adjacency matrix W into blocks. Here, for simplicity, we shall restrict our attention to the case of W having only four blocks:

$$W = \begin{pmatrix} W_{11} & W_{12} \\ W_{21} & W_{22} \end{pmatrix}.$$

Each block W_{nm} , $n, m = \overline{1, 2}$, represents a subgraph of the network in which the link density is characterized by z_{nm} , ie, which is generated via (2.1) and (2.2) using this z_{nm} . Among all possible topological block configurations, there are three distinct ones that we shall focus on: namely, the core–periphery as well as the modular assortative and disassortative structures (see Figure 1).

FIGURE 1 Examples of block structures obtained with the proposed models.

(a) Core–periphery structure, generated using (2.3) with $\phi = 1$. (b) Modular assortative structure ($\phi = 1, \lambda = 0.1$). (c) Modular disassortative structure ($\phi = 1, \beta = 0.1$). For all cases, we used $z = 10^{-9}$. In the top row, we report the heatmaps of the connection probability matrixes (with yellow and purple representing denser and sparser regions of the network, respectively). In the bottom row, we show the shape of a corresponding sample network. For the core–periphery case (part (a)), we display the core nodes (the top 20% biggest banks) in yellow and the peripheral nodes in violet. For the other two cases, the two colors refer to the two modules (of equal size).

2.3.1 Core–periphery topology

Of special interest in the investigation of financial networks is the core–periphery topology. Here, there are two groups of banks (core and periphery), with a much higher link density in the first group than in the second group as well as an intermediate link density between the two groups. As mentioned in the last section, the network generated by (2.1) inherently possesses a core–periphery structure. Therefore, further using a parameterization of the form $z_{11} = z, z_{12} = z_{21} = \gamma z, z_{22} = \gamma^2 z$, where $\gamma \in [0, 1]$, would already result in a core–periphery structure for $\gamma = 1$, with smaller values of γ simply marginalizing the peripheries. This is why we only use (2.3) to explore the transition between core–periphery and homogeneous topologies.

2.3.2 Assortative modular topology

In this case, the network is clustered into two groups of nodes (modules), with dense connections within the groups and sparse connections between them. This configuration corresponds to the choice of z_{11} and z_{22} both much larger than z_{12} and

z_{21} . Without loss of generality, we implement the assortative topology by setting $z_{11} = z_{22} = z$ and $z_{12} = z_{21} = \lambda z$, where $\lambda \in [0, 1]$.

2.3.3 Disassortative modular topology

As an opposing configuration to the assortative modular structure, one can consider the case in which the interconnections between the two modules dominate over the connections inside each module. The parameterization now is given by $z_{12} = z_{21} = z$ and $z_{11} = z_{22} = \beta z$, where $\beta \in [0, 1]$. Note that the limiting case $\beta \rightarrow 0$ corresponds to a purely bipartite structure.

We remark that for both the assortative and disassortative topologies we consider in this paper, each block is generated using (2.3) with the corresponding value of z_{nm} and with $\phi = 1$. As such, we have the signature of core–periphery structure within each module (as is clearly visible in Figure 1).

2.4 Shock propagation dynamics

Once a network instance is constructed, we use the Furfine and DebtRank algorithms to model the propagation of shocks on top of it (Bardoscia *et al* 2015, 2016; Furfine 2003).

2.4.1 Furfine algorithm

The Furfine algorithm can be expressed entirely as a function of equities, interacting through the liabilities network and with a given value of external assets or liabilities. The iterative map that represents the contagion dynamics is given by (Barucca *et al* 2016)

$$E_i(t + 1) = e_i + \sum_{j=1}^N A_{ij}(\Theta(E_j(t)) + R\Theta(-E_j(t))) - L_i, \quad (2.4)$$

where R is the exogenous recovery rate and e_i is the external net balance, which can be determined by looking at the initial discrepancy between the equity values and the interbank net balance.

In particular, for the data set under study, if the initial equity is larger or smaller than the net balance of interbank assets and liabilities, then this will imply the presence of a net external source of assets or liabilities, $e_i = E_i - A_i + L_i$.

From the iterative map, it is possible to define multiple measures of contagion loss. In particular, we will focus on one measure of contagion loss: the average relative equity loss, ie, we assume a relative shock to our set of banks, and we consider the shocked values as our initial value of the equity vector. Starting from this new equity vector, we identify the fixed point vector of the equity dynamics (2.4), E^* .

The average relative equity loss is then given by

$$\bar{E}_{\text{loss}} = \frac{\sum_i E_i^* - E_i(0)}{\sum_j E_j^{\text{pre}}}, \quad (2.5)$$

where the losses are computed relative to the initial pre-shock values, E_i^{pre} .

2.4.2 DebtRank

Alternatively, for a given step t of the dynamics, we consider the relative loss of equity $h_i(t)$ and the interbank leverage matrix $\Lambda_{ij}(t)$ of each bank i :

$$h_i(t) = \frac{E_i(0) - E_i(t)}{E_i(0)}, \quad (2.6)$$

$$\Lambda_{ij}(t) = \begin{cases} \frac{w_{i \rightarrow j}(0)}{E_i(0)} & \text{if bank } j \text{ has not defaulted up to time } (t-1), \\ 0 & \text{otherwise,} \end{cases} \quad (2.7)$$

where $E_i(0)$ is the initial equity of i . Assuming a loss given default of 100%, the dynamical equation for the relative equity loss $h_i(t)$ reads:

$$h_i(t+1) = \min \left[1, h_i(t) + \sum_{j=1}^N \Lambda_{ij}(t) [p_j^D(t+1) - p_j^D(t)] \right], \quad (2.8)$$

where $p_j^D(t) = h_j(t)e^{\alpha[h_j(t)-1]}$ is the probability of default of bank j at step t . The controlling parameter $\alpha \in (0, \infty)$ allows switching continuously from the linear DebtRank ($\alpha = 0$, meaning that the default probability is directly proportional to equity losses) (Bardoscia *et al* 2015) to the Furfine algorithm ($\alpha \rightarrow \infty$, ie, default occurs only when equity is depleted, and the bank is not contagious otherwise) (Furfine 2003). The average relative equity loss at the end of the shock propagation dynamics t^* is

$$\bar{E}_{\text{loss}} = \sum_i \frac{[h_i(t^*) - h_i(1)]E_i(0)}{\sum_j E_j(0)}, \quad (2.9)$$

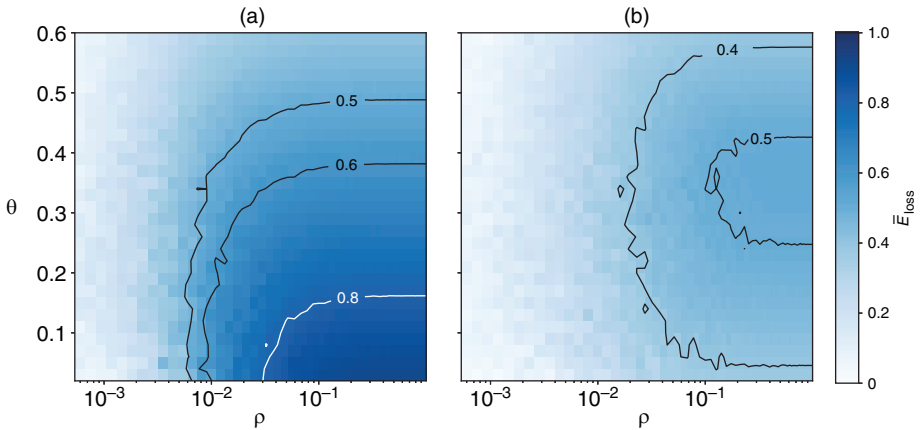
where $h_i(1)$ is the initial shock on i . Hence, \bar{E}_{loss} does not account for the initial shock on the system, but only for the network effect on systemic losses.

We use two kinds of stopping conditions for simulations: either when the difference $\|[h(t) - h(t-1)]E(0)\|_2$ becomes smaller than a tolerance $\text{tol} = 10^{-5}$, or when the number of interactions is equal to $\text{max}_{\text{iter}} = 10^5$.

3 RESULTS

As mentioned before, our operative framework consists of building an ensemble of interbank networks (using balance sheet data for either the year 2008 or the year

FIGURE 2 \bar{E}_{loss} (computed with linear DebtRank) as a function of the link density and the magnitude of the uniform shock, for core–periphery networks built with data from (a) 2008 and (b) 2013 using (2.3) with $\phi = 1$.



Darker (brighter) color refers to the higher (smaller) DebtRank, which corresponds to a more fragile (resilient) financial network.

2013) and then using the DebtRank shock propagation dynamics to run stress tests on each of these networks. \bar{E}_{loss} is the average outcome of the process over an ensemble of cardinality 100.

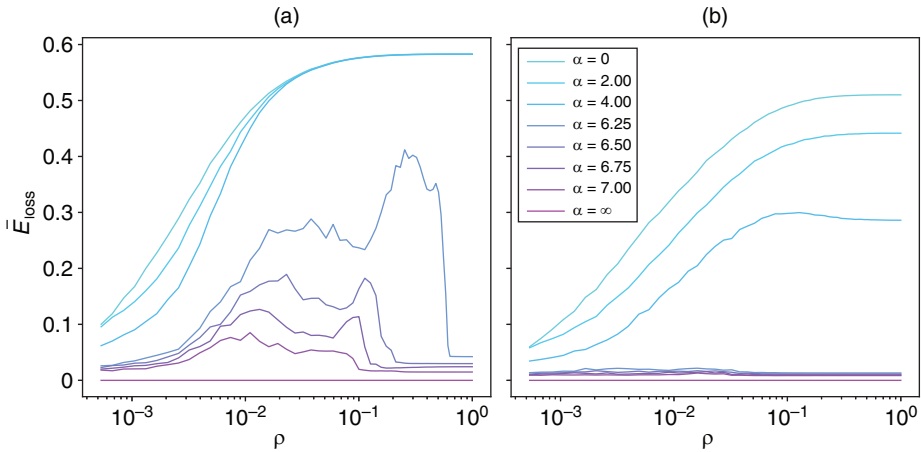
The first and most basic exercise we perform focuses on studying the standard fitness configuration model of Cimini *et al* (2015), generated using (2.3) with $\phi = 1$, and varying network density ρ . In terms of initial shock, we consider a uniform shock by reducing the equity of each bank by a fraction θ of its initial value, which means $h_i(1) = \theta$ for all i . Figure 2 shows the result of this exercise for ρ ranging from 0 to 1 and θ ranging from 0 to 0.6. We see that \bar{E}_{loss} increases monotonically with ρ . This implies that the network becomes more fragile when it becomes more dense, which is consistent with the findings of Bardoscia *et al* (2017). In 2008, we find a very high value of \bar{E}_{loss} for very small θ : network amplification effects are so important that they can wipe out the whole system when the initial perturbation is minimal. The decreasing of \bar{E}_{loss} with θ is instead mainly due to the fact that initial shocks are not included in the computation of \bar{E}_{loss} , and indeed this quantity is bounded from above by $1 - \theta$. Finally, by comparing the 2008 data and the 2013 data, we find that the \bar{E}_{loss} for every combination of ρ and θ has substantially changed: the network is much more robust in 2013 than in 2008, especially for what concerns small shocks (even in the high density regime) (Cimini and Serri 2016).

Note that in this exercise we have looked at the case of linear DebtRank, which corresponds to the choice $\alpha = 0$ in (2.8). We now perform an analogous exercise but looking at different values of α . In particular, we are interested in the cases of DebtRank, Furfine and the nonlinear default probability in between. To this end, we consider in Figure 3 the values $\alpha = 0, 2, 4, 6.25, 6.5, 6.75, 7, \infty$. This set of parameters was chosen so that the reader can see a clear transition in \bar{E}_{loss} behavior but, at the same time, the number of curves is small enough for the plot to be readable. Concerning 2008 networks, in general, for small α , we see that \bar{E}_{loss} increases with ρ and converges toward the highest value of $\bar{E}_{\text{loss}} = 1 - \theta$. In contrast, for large α , equity losses due to the network remain very small for both very dense and very sparse networks, and they attain a maximum for intermediate density values. The transition between these two regimes appears around the case $\alpha = 5$, corresponding to a highly nonlinear default probability. Moving to 2013 networks, the increasing behavior of \bar{E}_{loss} with ρ is also generally observed in this case; however, \bar{E}_{loss} for completely connected networks does depend on the value of α . The regime of nonlinear default probability shows very moderate losses, in line with the interpretation that in 2013 the interbank market was much more stable than in 2008.

The flat, and equal to zero, curve for the $\alpha = \infty$ case is a technical consequence of using homogeneous shocks with Furfine. To address this issue, in addition to the uniform shock, we study the effect of defaulting a single bank either from the core or from the periphery. In the latter case, we divide all the banks into core, middle and periphery (with around thirty banks in each group) by ordering them according to their reconstructed degree, ie, to their exposure (as a consequence of the fitness ansatz used in the reconstruction procedure). Then we choose to default one of them randomly and average the result over 100 picks from a given group. As shown in Figure 4, the behavior of \bar{E}_{loss} is significantly different for core and periphery shocks. The latter result in either an increase of the risk as a function of density for $\alpha = 0$ (linear case) or a decrease when $\alpha > 0$. When shocking the core, however, we observe an increase of risk for small densities, but at some point it reaches a maximum and then drops (nonlinear case) or remains at the same level (linear case). In addition, Figure 5 shows how this dependence is affected by the recovery rate R in the Furfine case. Obviously, the losses are decreased with increasing R , but the overall function form does not change. Although qualitatively 2008 and 2013 are very similar, 2013 is more robust for all analyzed cases.

Up to this point, we have considered core–periphery interbank network structures generated using (2.3) with $\phi = 1$. We now consider other values of ϕ , up to the case $\phi = 0$ corresponding to an Erdős–Rényi topology. Figure 6 shows network losses \bar{E}_{loss} as a function of ϕ and for different types of initial shocks. We see that uniform shocks cause a loss that is increasing with ϕ , so the more core–periphery

FIGURE 3 \bar{E}_{loss} as a function of the link density for a fixed value $\theta = 0.4$ of uniform initial shock, for networks built with data from (a) 2008 and (b) 2013 using (2.3) with $\phi = 1$.

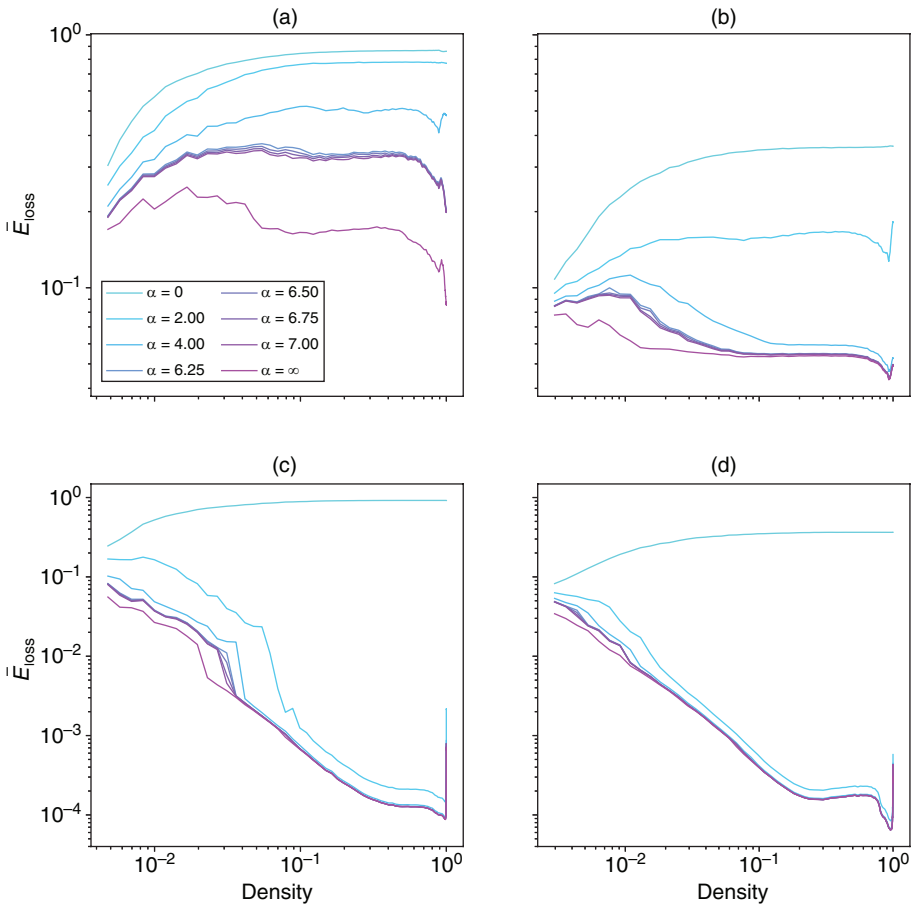


Different curves correspond to different magnitudes of nonlinearity in the DebtRank default probabilities entering in (2.8).

the structure, the more fragile the system is. This behavior is observed for different values of the network density and for both 2008 and 2013. Moreover, as we already observed in Figure 2, small uniform shocks cause higher relative losses than bigger ones in 2008, whereas the opposite is true in 2013. One should note, however, that if we sum the relative loss and the initial loss, such a sum is always higher for a higher initial shock. In addition, 2013 is much more robust with \bar{E}_{loss} not exceeding 0.5 even for $\phi = 1.0$ and $\theta = 0.3$.

Interestingly, the behavior changes when we consider single bank defaults. When the network is more random ($\phi \sim 0$), both types of shock result in a similar value of \bar{E}_{loss} . Yet, as the distinction between core and periphery emerges and becomes more marked, the result of shocking either of them changes. As can be seen in all four panels of Figure 6, shocking the periphery is almost equivalent to the small uniform shock scenario. Indeed, the average initial shock corresponding to a single bank default in the periphery is around 0.1% of the whole initial equity. Having said that, the loss induced by defaulting a bank belonging to the core is not an increasing function of ϕ . For denser networks, with $\rho = 0.15$, it decreases in the near random regime and then stays constant. In the case of $\rho = 0.05$, \bar{E}_{loss} reaches a minimum and then increases with ϕ . The existence of an optimal ϕ , from a core defaults perspective, is an important observation from a regulatory point of view. Note that the

FIGURE 4 \bar{E}_{loss} as a function of the link density for point initial shocks in (a), (b) the core or (c), (d) the periphery, for networks built with data from (a), (c) 2008 and (b), (d) 2013 using (2.3) with $\phi = 1$.

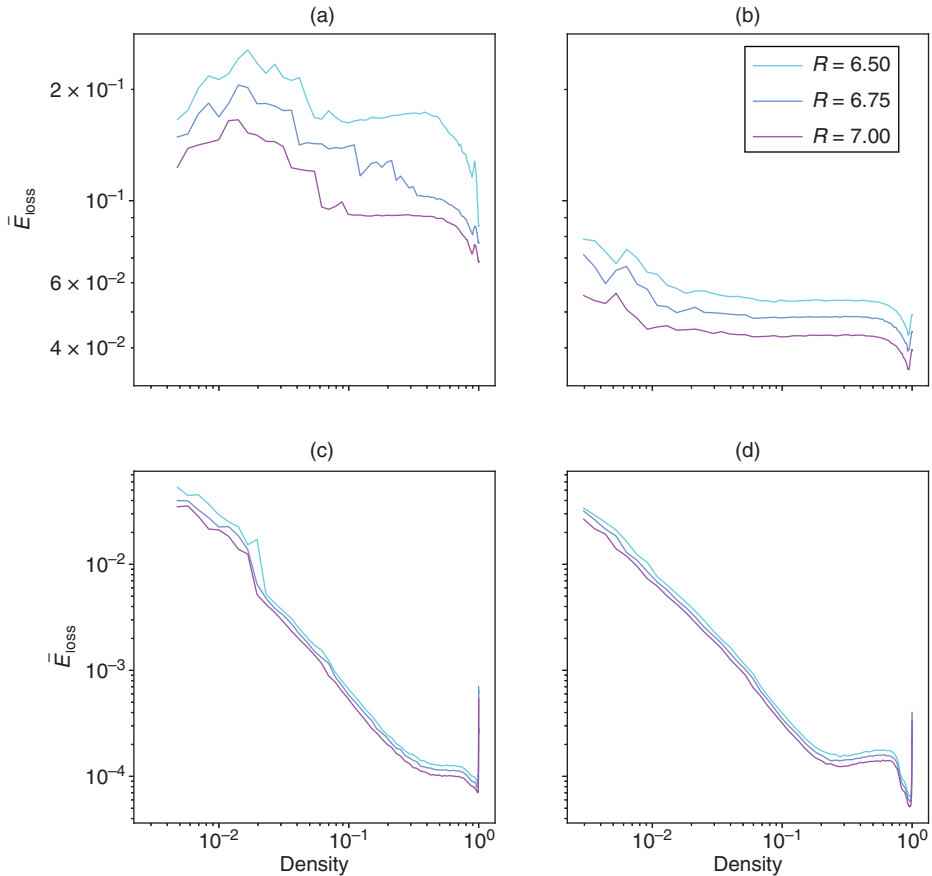


Different curves correspond to different magnitudes of nonlinearity in the default probabilities entering in (2.8).

average initial loss corresponding to the default of a core bank is more than 4% of the entire system equity.

We finally consider the modular assortative and disassortative topologies, by varying the structural parameters λ and β but for fixed $\phi = 1$. Figure 7 shows the results of an exercise in which we uniformly shock banks from the first module and measure \bar{E}_{loss} for the second module. We observe that the assortative structure can be quite resilient if the different blocks are scarcely connected. However, above a

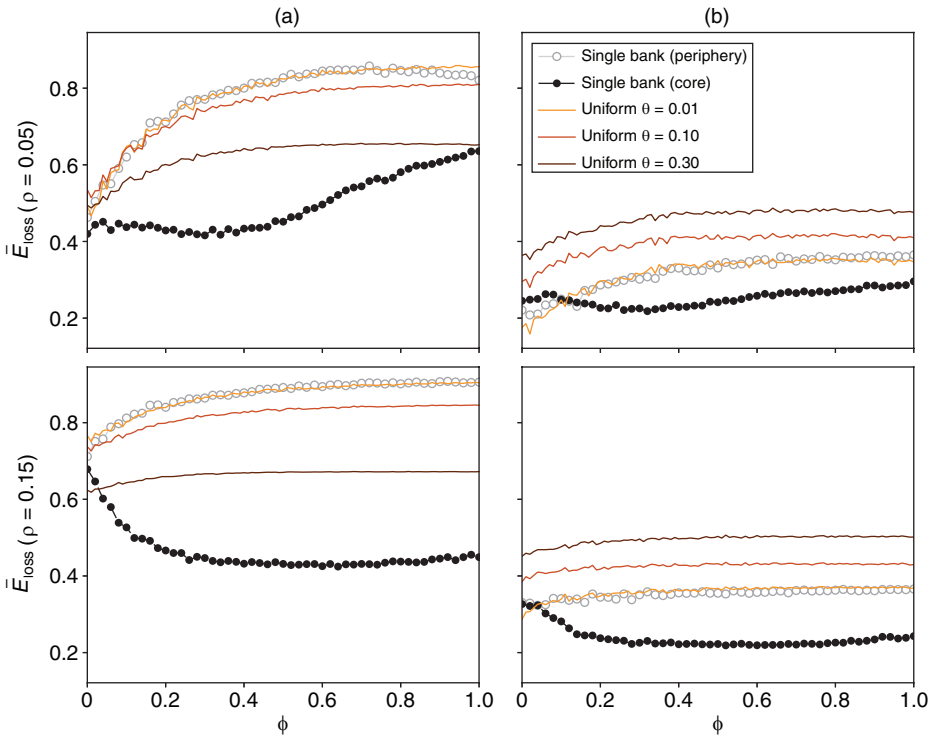
FIGURE 5 \bar{E}_{loss} for the Furfine model as a function of the link density for point initial shocks in (a), (b) the core or (c), (d) the periphery, for networks built with data from (a), (c) 2008 and (b), (d) 2013 using (2.3) with $\phi = 1$.



Different curves correspond to different values of the exogenous recovery rate R .

given value of λ the structure becomes almost as fragile as in the case without the blocks ($\lambda = 1$). Concerning disassortative structures, systemic risk decreases when we move away from a pure bipartite structure. The differences are relatively small though, and there is no jump similar to the one observed for assortative structures. For a constant density, this may be the result of a decreasing number of connections between the two groups when we increase β . In this way, the losses are not transmitted to the other side as quickly as in the purely bipartite case. Qualitatively similar results were obtained for the 2013 data.

FIGURE 6 \bar{E}_{loss} (computed with linear DebtRank) as a function of the parameter ϕ of (2.3) tuning the strength of the core–periphery structure, for both (a) 2008 and (b) 2013 interbank networks.



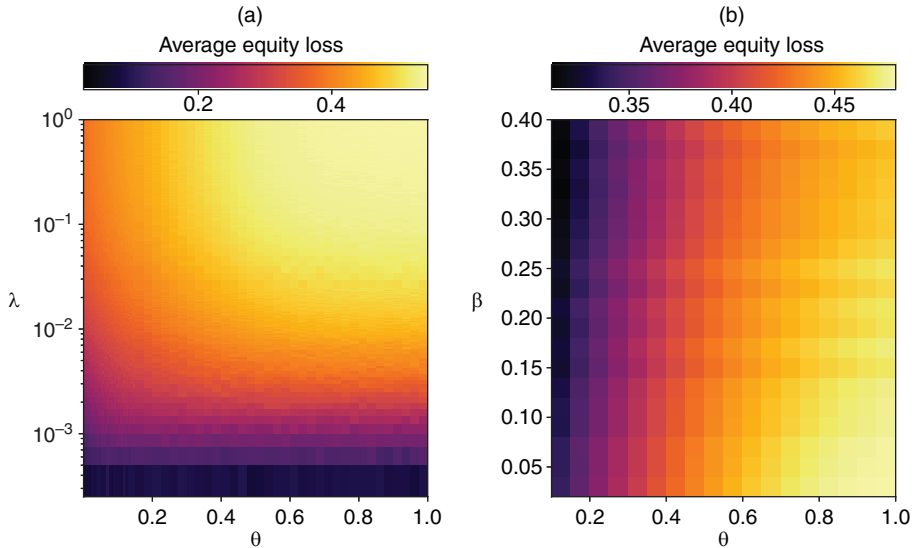
We consider fixed values of the density $\rho = 0.05$ (top two panels) and $\rho = 0.15$ (bottom two panels) as well as different initial shocks: either uniform for all banks, or consisting of a single initial default (in the core or in the periphery).

4 DISCUSSION

In this work, we have examined different structures of the interbank network and have shown how they affect systemic risk. In addition, we have used a variety of shock types and changed the way they propagate across the network. These results provide additional evidence of how complex the interbank system is and how many variables are involved in determining its resilience.

In the simplest situation of a single-block network with a core–periphery structure, systemic risk monotonically increases with density, but there is a quantitative difference between the behavior observed in 2008 and 2013: the crisis (and the consequent regulatory interventions) shaped banks' balances in such a way that, afterward, the

FIGURE 7 \bar{E}_{loss} (computed with linear DebtRank) as a function of the uniform initial shock θ and model parameter λ and β of the modular (a) assortative and (b) disassortative topological structure, respectively.



In both cases, $\phi = 1$ and $\rho = 0.1$, and the interbank networks refer to the year 2008.

interbank market became much more robust to small shocks even in the high density regime.

Our analysis of the different shapes of bank default probability further shows the differences between the pre- and postcrisis landscape. In 2008, there are basically two regimes of shock propagation, depending on the network density and the parameter α , which can also be seen as the amount of confidence market participants have in the ability of counterparties to recover from equity losses. Indeed, if the confidence in the system is not high enough, systemic losses become widespread; otherwise, they remain small. In 2013, however, even for low confidence levels, increasing the density does not lead to overall losses equal to those observed for the linear case (ie, that corresponding to the lowest level of trust in the counterparty). Note that these results were obtained with uniform shocks across all banks. As shown in Mastromatteo *et al* (2012), if we consider the defaults of single banks as initial shocks, then we might expect that increasing the density will help the system to withstand the shock.

As a matter of fact, the core–periphery structure is naturally generated by the network (re)construction method described by (2.1), where assets and liabilities are

shown to have fat-tailed distributions. In this scenario, the only topological parameter that can be tuned is the network density, which allows us to switch from networks with a few contracts of large amounts to networks with many contracts of small amounts. However, by introducing the parameter ϕ in (2.3), we were also able to continuously change the network structure from a random one ($\phi = 0$) to a core–periphery one ($\phi = 1$). We then found that the core–periphery structure is less resilient, at least for uniform shocks. This confirms the well-known observation that strongly connected nodes enhance shock propagation (Hüser 2015).

For the data set under study, default contagion algorithms (ie, Furfine or DebtRank for $\alpha \rightarrow \infty$) would not yield any equity losses for uniform shocks, ie, no propagation occurs unless a bank actually defaults. Meanwhile, distress contagion algorithms (ie, DebtRank for finite α) distinguished between the vulnerabilities of different institutions before any default occurred.

In the case of initial bank defaults, the propagation depends on whether the defaults appeared in the core or in the peripheries. The peripheries are clearly more fragile, as the structure becomes more core–periphery than random. Importantly, the core is quite robust, especially between the two extreme structures. In this case, both default and distress contagion algorithms display equity losses.

In the last step of our analysis, we looked at the block structure of the network. On the one hand, we found that an assortative modular structure can faithfully represent a market of several countries, in which home and foreign connectivities are different (the former being typically much larger). On the other hand, the disassortative modular case is often observed in financial networks, especially at a low data aggregation scale for which a bank is either a lender or a borrower, but not both (Barucca and Lillo 2016). In both cases, we showed how a shock originating in one block propagates to another. For the assortative case, we observed a significant jump in systemic risk above some given density of connections between the blocks. The disassortative structure, however, does not reveal any kind of similar discontinuity. Nevertheless, moving away from the pure bipartite case slowly decreases the systemic risk.

Overall, we showed that the outcome of a systemic event is very much dependent on the details of both the underlying network and shock propagation. We believe this observation is relevant for more general frameworks such as multilayer financial networks (Bargigli *et al* 2015; Battiston and Martínez-Jaramillo 2018; Poledna *et al* 2015) and networks of portfolio holdings (Caccioli *et al* 2014; Cont and Wagalath 2016; Greenwood *et al* 2015; Gualdi *et al* 2016; Pichler *et al* 2018). Our results may thus inspire more in-depth analyses, and may provide useful insights to regulators in trying to shape a more resilient financial system. In the latter case, knowledge about the systemic consequences of changing the interbank network density or reshaping its structure would be valuable in arguments either for or against a given solution.

Moreover, studying the effects caused by different shock propagation types can help in predicting the outcomes of different stress scenarios.

DECLARATION OF INTEREST

The authors report no conflicts of interest. The authors alone are responsible for the content and writing of the paper.

ACKNOWLEDGEMENTS

This work is the output of the first Complexity72h workshop, held at IMT School in Lucca, May 7–11, 2018. See <https://complexity72h.weebly.com/>.

REFERENCES

- Acemoglu, D., Ozdaglar, A., and Tahbaz-Salehi, A. (2015). Systemic risk and stability in financial networks. *American Economic Review* **105**(2), 564–608 (<https://doi.org/10.1257/aer.20130456>).
- Acharya, V. V., Pedersen, L. H., Philippon, T., and Richardson, M. (2017). Measuring systemic risk. *Review of Financial Studies* **30**(1), 2–47 (<https://doi.org/10.1093/rfs/hhw088>).
- Allen, F., and Gale, D. (2007). Systemic risk and regulation. In *The Risks of Financial Institutions*, pp. 341–376. University of Chicago Press.
- Allen, F., Hryckiewicz, A., Kowalewski, O., and Tümer-Alkan, G. (2014). Transmission of financial shocks in loan and deposit markets: role of interbank borrowing and market monitoring. *Journal of Financial Stability* **15**, 112–126 (<https://doi.org/10.1016/j.jfs.2014.09.005>).
- Amini, H., Cont, R., and Minca, A. (2016). Resilience to contagion in financial networks. *Mathematical Finance* **26**(2), 329–365 (<https://doi.org/10.1111/mafi.12051>).
- Anand, K., van Lelyveld, I., Banai, A., Christiano Silva, T., Friedrich, S., Garratt, R., Halaj, G., Hansen, I., Howell, B., Lee, H., Martínez Jaramillo, S., Molina-Borboa, J., Nobili, S., Rajan, S., Rubens Stancato de Souza, S., Salakhova, D., and Silvestri, L. (2018). The missing links: a global study on uncovering financial network structure from partial data. *Journal of Financial Stability* **35**, 107–119 (<https://doi.org/10.1016/j.jfs.2017.05.012>).
- Angelini, P., Nobili, A., and Picillo, C. (2011). The interbank market after August 2007: what has changed, and why? *Journal of Money, Credit and Banking* **43**(5), 923–958 (<https://doi.org/10.1111/j.1538-4616.2011.00402.x>).
- Bardoscia, M., Battiston, S., Caccioli, F., and Caldarelli, G. (2015). Debtrank: a microscopic foundation for shock propagation. *PLoS ONE* **10**(6), e0130406 (<https://doi.org/10.1371/journal.pone.0130406>).
- Bardoscia, M., Caccioli, F., Perotti, J. I., Vivaldo, G., and Caldarelli, G. (2016). Distress propagation in complex networks: the case of non-linear debtrank. *PLoS ONE* **11**(10), e0163825 (<https://doi.org/10.1371/journal.pone.0163825>).

- Bardoscia, M., Battiston, S., Caccioli, F., and Caldarelli, G. (2017). Pathways towards instability in financial networks. *Nature Communications* **8**, 14416 (<https://doi.org/10.1038/ncomms14416>).
- Bardoscia, M., Barucca, P., Codd, A. B., and Hill, J. (2019). Forward-looking solvency contagion. *Journal of Economic Dynamics and Control* **108**, 103755.
- Bargigli, L., di Iasio, G., Infante, L., Lillo, F., and Pierobon, F. (2015). The multiplex structure of interbank networks. *Quantitative Finance* **15**(4), 673–691 (<https://doi.org/10.1080/14697688.2014.968356>).
- Barucca, P., and Lillo, F. (2016). Disentangling bipartite and core–periphery structure in financial networks. *Chaos, Solitons and Fractals* **88**, 244–253 (<https://doi.org/10.1016/j.chaos.2016.02.004>).
- Barucca, P., Bardoscia, M., Caccioli, F., D’Errico, M., Visentin, G., Battiston, S., and Caldarelli, G. (2016). Network valuation in financial systems. Preprint (arXiv:1606.05164).
- Battiston, S., Caldarelli, G., D’Errico, M., and Gurciullo, S. (2016a). Leveraging the network: a stress-test framework based on debrank. *Statistics and Risk Modeling* **33**(3–4), 117–138 (<https://doi.org/10.1515/strm-2015-0005>).
- Battiston, S., Farmer, J. D., Flache, A., Garlaschelli, D., Haldane, A. G., Heesterbeek, H., Hommes, C., Jaeger, C., May, R., and Scheffer, M. (2016b). Complexity theory and financial regulation. *Science* **351**(6275), 818–819 (<https://doi.org/10.1126/science.aad0299>).
- Battiston, S., and Martínez-Jaramillo, S. (2018). Financial networks and stress testing: challenges and new research avenues for systemic risk analysis and financial stability implications. *Journal of Financial Stability* **35**, 6–16 (<https://doi.org/10.1016/j.jfs.2018.03.010>).
- Battiston, S., Puliga, M., Kaushik, R., Tasca, P., and Caldarelli, G. (2012). Debrank: too central to fail? financial networks, the fed and systemic risk. *Scientific Reports* **2**, 541 (<https://doi.org/10.1038/srep00541>).
- Benoit, S., Colliard, J.-E., Hurlin, C., and Pérignon, C. (2017). Where the risks lie: a survey on systemic risk. *Review of Finance* **21**(1), 109–152 (<https://doi.org/10.1093/rof/rfw026>).
- Boss, M., Elsinger, H., Summer, M., and Thurner, S. (2004). Network topology of the interbank market. *Quantitative Finance* **4**(6), 677–684 (<https://doi.org/10.1080/14697680400020325>).
- Caccioli, F., Shrestha, M., Moore, C., and Farmer, J. D. (2014). Stability analysis of financial contagion due to overlapping portfolios. *Journal of Banking and Finance* **46**, 233–245 (<https://doi.org/10.1016/j.jbankfin.2014.05.021>).
- Caccioli, F., Barucca, P., and Kobayashi, T. (2018). Network models of financial systemic risk: a review. *Journal of Computational Social Science* **1**(1), 81–114 (<https://doi.org/10.1007/s42001-017-0008-3>).
- Cimini, G., and Serri, M. (2016). Entangling credit and funding shocks in interbank markets. *PLoS ONE* **11**(8), e0161642 (<https://doi.org/10.1371/journal.pone.0161642>).
- Cimini, G., Squartini, T., Garlaschelli, D., and Gabrielli, A. (2015). Systemic risk analysis on reconstructed economic and financial networks. *Scientific Reports* **5**, 15758 (<https://doi.org/10.1038/srep15758>).
- Cimini, G., Squartini, T., Saracco, F., Garlaschelli, D., Gabrielli, A., and Caldarelli, G. (2019). The statistical physics of real-world networks. *Nature Reviews Physics* **1**(1), 58–71 (<https://doi.org/10.1038/s42254-018-0002-6>).

- Cocco, J. F., Gomes, F. J., and Martins, N. C. (2009). Lending relationships in the inter-bank market. *Journal of Financial Intermediation* **18**(1), 24–48 (<https://doi.org/10.1016/j.jfi.2008.06.003>).
- Cont, R., and Wagalath, L. (2016). Fire sales forensics: measuring endogenous risk. *Mathematical Finance* **26**(4), 835–866 (<https://doi.org/10.1111/mafi.12071>).
- Covi, G., Montagna, M., and Torri, G. (2019). Economic shocks and contagion in the euro area banking sector: a new micro-structural approach. Financial Stability Review, May, European Central Bank. URL: <https://bit.ly/31g6mCq>.
- Eisenberg, L., and Noe, T. H. (2001). Systemic risk in financial systems. *Management Science* **47**(2), 236–249 (<https://doi.org/10.2139/ssrn.173249>).
- Furfine, C. (2003). Interbank exposures: quantifying the risk of contagion. *Journal of Money, Credit, and Banking* **35**(1), 111–128 (<https://doi.org/10.1353/mcb.2003.0004>).
- Gai, P., and Kapadia, S. (2010). Contagion in financial networks. *Proceedings of the Royal Society of London A* **466**, 2401–2423 (<https://doi.org/10.1098/rspa.2009.0410>).
- Georg, C.-P. (2013). The effect of the interbank network structure on contagion and common shocks. *Journal of Banking and Finance* **37**(7), 2216–2228 (<https://doi.org/10.1016/j.jbankfin.2013.02.032>).
- Greenwood, R., Landier, A., and Thesmar, D. (2015). Vulnerable banks. *Journal of Financial Economics* **115**(3), 471–485 (<https://doi.org/10.1016/j.jfineco.2014.11.006>).
- Gualdi, S., Cimini, G., Primicerio, K., Clemente, R. D., and Challet, D. (2016). Statistically validated network of portfolio overlaps and systemic risk. *Scientific Reports* **6**, 39467 (<https://doi.org/10.1038/srep39467>).
- Haldane, A. G., and May, R. M. (2011). Systemic risk in banking ecosystems. *Nature* **469**, 351–355 (<https://doi.org/10.1038/nature09659>).
- Hurd, T. R., Gleeson, J. P., and Melnik, S. (2017). A framework for analyzing contagion in assortative banking networks. *PLoS ONE* **12**(2), e0170579 (<https://doi.org/10.1371/journal.pone.0170579>).
- Hüser, A.-C. (2015). Too interconnected to fail: a survey of the interbank networks literature. *The Journal of Network Theory in Finance* **1**(3), 1–50 (<https://doi.org/10.21314/JNTF.2015.001>).
- Krause, S. M., Štefančić, H., Zlatić, V., and Caldarelli, G. (2019). Controlling systemic risk – network structures that minimize it and node properties to calculate it. Preprint (arXiv: 1902.08483).
- León, C., and Berndsen, R. J. (2014). Rethinking financial stability: challenges arising from financial networks' modular scale-free architecture. *Journal of Financial Stability* **15**, 241–256 (<https://doi.org/10.1016/j.jfs.2014.10.006>).
- Mastromatteo, I., Zarinelli, E., and Marsili, M. (2012). Reconstruction of financial networks for robust estimation of systemic risk. *Journal of Statistical Mechanics: Theory and Experiment* **2012**(03), P03011 (<https://doi.org/10.1088/1742-5468/2012/03/P03011>).
- Montagna, M., and Lux, T. (2017). Contagion risk in the interbank market: a probabilistic approach to cope with incomplete structural information. *Quantitative Finance* **17**(1), 101–120 (<https://doi.org/10.1080/14697688.2016.1178855>).
- Nier, E. W., Yang, J., Yorulmazer, T., and Alentorn, A. (2007). Network models and financial stability. *Journal of Economic Dynamics and Control* **31**(6), 2033–2060 (<https://doi.org/10.1016/j.jedc.2007.01.014>).

- Pichler, A., Poledna, S., and Thurner, S. (2018). Systemic-risk-efficient asset allocation: minimization of systemic risk as a network optimization problem. Preprint (arXiv: 1801.10515).
- Poledna, S., Molina-Borboa, J. L., Martínez-Jaramillo, S., van der Leij, M., and Thurner, S. (2015). The multi-layer network nature of systemic risk and its implications for the costs of financial crises. *Journal of Financial Stability* **20**, 70–81 (<https://doi.org/10.1016/j.jfs.2015.08.001>).
- Roukny, T., Bersini, H., Pirotte, H., Caldarelli, G., and Battiston, S. (2013). Default cascades in complex networks: topology and systemic risk. *Scientific Reports* **3**, 2759 (<https://doi.org/10.1038/srep02759>).
- Squartini, T., Cimini, G., Gabrielli, A., and Garlaschelli, D. (2017). Network reconstruction via density sampling. *Applied Network Science* **2**(1), 3 (<https://doi.org/10.1007/s41109-017-0021-8>).
- Squartini, T., Caldarelli, G., Cimini, G., Gabrielli, A., and Garlaschelli, D. (2018). Reconstruction methods for networks: the case of economic and financial systems. *Physics Reports* **757**, 1–47 (<https://doi.org/10.1016/j.physrep.2018.06.008>).